

Measurement of the Electric Polarizability of the Neutron

J. Schmiedmayer, H. Rauch, and P. Riehs

Institut für Kernphysik, Technische Universität Wien, A-1040 Wien, Austria

(Received 19 April 1988)

At the HELIOS neutron source in Harwell, the neutron transmission of Pb and C was very precisely measured within the $50 \text{ eV} < E < 50 \text{ keV}$ energy range, with use of a 150-m flight path, newly developed time-of-flight electronics, and a ^{10}B -loaded liquid scintillator. After correction for neutron-electron, Schwinger, and resonance scattering, the electric polarizability of the neutron was determined to be $\alpha_n = (1.2 \pm 1.0) \times 10^{-3} \text{ fm}^3$ from the energy dependence of the total scattering cross section.

PACS numbers: 13.40.Fn, 14.20.Dh, 25.40.Dn

Because of its internal structure, the neutron has an extended charge distribution, which should be polarizable in an external electric field. The induced electric dipole moment \mathbf{D} is given by the well-known relation $\mathbf{D} = 4\pi\epsilon_0\alpha\mathbf{E}$, where α is the electric polarizability.

The electric polarizability of the neutron α_n can be estimated from quark models.¹ Values of the order of $1 \times 10^{-3} \text{ fm}^3$ were obtained for the neutron and the proton. The sum of the dynamic electric $\bar{\alpha}$ and magnetic $\bar{\beta}$ polarizabilities can be estimated² from photoabsorption cross-section measurements above threshold with forward sum rules [$\bar{\alpha} + \bar{\beta} = (14.2 \pm 0.3) \times 10^{-4} \text{ fm}^3$]. From single-pion photoproduction, limits of $5 \times 10^{-4} \text{ fm}^3 < \bar{\alpha}_n < 14 \times 10^{-4} \text{ fm}^3$ were obtained.³ In a further semitheoretical analysis of the total photoabsorption cross sections of the neutron and the proton, a value of $\alpha_n = 8.5 \times 10^{-4} \text{ fm}^3$ was calculated which depends on the model and nucleon form factors.⁴

The smallness of α_n makes a measurement with macroscopic electric fields of present technology rather impossible. In the microscopic field of a nucleus the interaction potential, due to α_n , is given by $V_{\text{pot}} = -\frac{1}{2}\alpha_n Z^2 e^2/r^4$. The corresponding scattering amplitude was first calculated by Thaler⁵ and by Breit and Rustgi.⁶ Its overall contribution to the neutron-atom scattering is nearly proportional to $Z^{5/3}$. For $\alpha_n = 1 \times 10^{-3} \text{ fm}^3$ and $Z = 82$, about 0.5% of the scattering length and 1% of the scattering cross section are induced by α_n . This is of the same order of magnitude as the

well-established neutron-electron interaction,⁷ and large compared to the accuracy of $\Delta b/b \approx 2 \times 10^{-4}$ obtained in thermal-neutron scattering-length measurements.⁸ The energy dependence is small and stems mainly from a term proportional to the momentum transfer $\hbar q$, which is characteristic for the $1/r^4$ interaction potential. Previous experiments based on differential⁹ ($\alpha_n < 6.1 \times 10^{-3} \text{ fm}^3$) or total¹⁰ scattering cross-section measurements [$\alpha_n = (3 \pm 4) \times 10^{-3} \text{ fm}^3$] gave only upper limits or contradictory results¹¹: [$\alpha_n = (260 \pm 100) \times 10^{-3} \text{ fm}^3$].

In this Letter we will present a new measurement of α_n , using explicitly the characteristic q dependence of the scattering amplitude. All electromagnetic effects in non-magnetic atoms were included in a rigorous calculation within the first Born approximation. The neutron-atom scattering cross section up to 100-keV neutron energy was calculated, including all interference terms between different interactions.¹² The nucleus was assumed to be a homogeneously charged sphere with radius R_N and total charge Z . A simple exponential model for the electron cloud, electron form factors from Ref. 13, and relativistic Hartree-Fock calculations¹⁴ were used. Potential and resonance scattering were considered for the neutron-nucleus interaction and Schwinger scattering, neutron-electron interaction, and electric polarizability for the electric interactions of the neutron. It was shown that the nuclear charge distribution and its electric field dominate the scattering amplitude of α_n . The effect of the electron cloud can be neglected.¹² The scattering amplitude for $qR_N \ll 1$ is given by^{12,15}

$$f(q) = \alpha_n Z^2 \frac{e^2 m}{\hbar^2} \frac{1}{R_N} \left[\frac{6}{5} - \frac{\pi}{4} q R_N + \frac{4}{7} (q R_N)^2 - \frac{1}{540} (q R_N)^4 \dots \right]. \quad (1)$$

As has been described in detail in Ref. 12, the shape of the total scattering cross section σ_s can be parametrized by

$$\sigma_s(k) = \sigma_s(0) + ak + bk^2 + O(k^4), \quad (2)$$

where $k = 2.1968 \times 10^{-4} \sqrt{EA}/(A+1)$ (k in fm^{-1} and E in eV) is the wave vector of the incoming neutron. The parameter a depends only on α_n . b comes mainly from

the effective range of the neutron-nucleus interaction. The effect due to α_n on the scattering cross section is best demonstrated by our defining D as

$$D(k) = \frac{1}{k} \frac{\sigma_s(0) - \sigma_s(k)}{\sigma_s(0)} = A + Bk + O(k^3). \quad (3)$$

In the region $E < 20 \text{ keV}$, the characteristic term pro-

portional to the momentum $\hbar k$ of the incoming neutron in Eq. (2) can be separated from effective-range effects ($\propto k^2$) in neutron-nucleus scattering. An accuracy of 1 part in 500 is necessary for fifty measured cross-section points in the energy range 50 eV to 20 keV to achieve an error of 10^{-3} fm^3 in α_n . Since only the energy dependence of the total scattering cross section is important, most of the normalization problems are avoided by measurement of $\sigma_s(E)$ over the whole energy range in one experiment.

The aim of our experiment was to determine simultaneously the values for a and b of Eq. (2) from the shape of the neutron-scattering sections. More details of the experiment and the data evaluation are described in Ref. 12. The shape was measured with a transmission setup with the 150-m flight path at the fast-neutron target of the HELIOS neutron source at Harwell (see inset of Fig. 1). Natural Pb was chosen because it is the only heavy element with few widely spaced narrow resonances. ^{208}Pb (52.4% abundance) has no known resonances below 40 keV and no s -wave resonances below 200-keV neutron energy. ^{207}Pb (22.1% abundance) shows a large s -wave resonance at 42 keV, a level near -36 keV, and, like ^{204}Pb (1.4% abundance) and ^{206}Pb (24.1% abundance), some smaller resonances which have to be taken into account.^{17,18} The systematic errors due

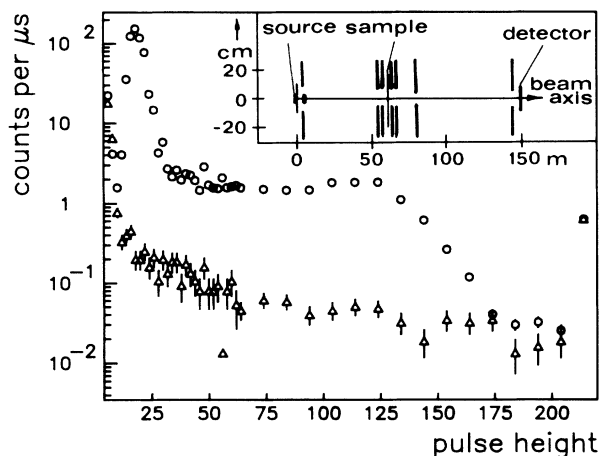


FIG. 1. Pulse-height spectrum of the ^{10}B -loaded liquid scintillator selected at 5-keV neutron energy from the two-dimensional pulse-height time-of-flight histogram, measured with the flash analog-to-digital converter electronics (Ref. 16). For neutrons (circles), the α peak of the $^{10}\text{B}(n,\alpha)^7\text{Li}$ reaction and the Compton edge from the 480-keV γ rays converting with about 15% probability in the detector are clearly seen. The γ -ray background (triangles) was measured with a 65-mm-thick polyethylene filter. At the α peak, a signal-to-background ratio of better than 300:1 is reached. The shape of the time-dependent background can be estimated from the low and high pulse-height channels. Inset: a sketch of the measurement geometry.

to the resonance correction can be reduced to a very low level, by our making a simultaneous determination of the resonance parameters. Carbon was chosen as a test case for its low Z and flat cross section. The effect induced by α_n should be negligible.

To obtain the required accuracy, a fast 10-ns dead-time multiparameter time-of-flight system was developed,¹⁶ with fast emitter-coupled logic and a 100-MHz flash analog-to-digital converter for the analog signal measurement. Detector variations, bias shifts, and other irregularities are easily recognized in the two-dimensional pulse-height time-of-flight histograms.

Commercially available ^{10}B -loaded liquid scintillators were used as neutron detectors. They have very high neutron detection efficiencies ϵ_n , low γ -ray sensitivity ϵ_γ , and sufficient time resolution. In the energy range 50 eV to 20 keV, the ratio $\epsilon_n/\epsilon_\gamma$ is by a factor of 5 to 10 better than that achieved with ^6Li -glass detectors.¹⁹ Typical signal-to-background ratios were up to 300:1 in the keV region (Fig. 1) and better than 100:1 over the whole energy range.

Data were taken in three periods of 6 days, with the HELIOS electron linac running on 150-Hz and 50-ns pulse width. Samples with transmissions ranging from 50% down to 2% were measured. A moderator containing B and an additional ^{10}B filter decreased the neutron flux below 10 eV and reduced the corrections for neutrons overlapping between machine cycles. The background (typically $< 1\%$) was evaluated by thick resonance filters, a polyethylene absorber, and the known detector pulse-height distribution. All background data are well described by a simple model, including γ -ray transmission coefficients for different filters and samples. After dead-time and background correction, the transmission was calculated and an energy-dependent vacuum correction ($\approx 0.12\%$ for a $n\sigma = 1$ sample) was applied.

The detector time-of-flight resolution function was determined from the shape of the well-known resonances of ^{238}U , Co, Mn, W, using the REFIT²⁰ computer code. The whole data set for Pb was then analyzed with REFIT and new very accurate parameters for Γ_n were extracted which differ, in some cases by up to 10% and more, from values found in the literature.¹⁷ With the new parameter set the absorption and scattering cross section of each isotope was correctly reproduced from the same potential scattering radius, $R_0 = 9.73$ fm, for all isotopes. For the thermal incoherent scattering cross section we obtained 2.7 mb, which is in good agreement with the measured value of 3.0(7) mb.²¹ Including all resolution effects, the resonance corrections were calculated by subtraction of the theoretical transmissions with and without resonances for each time-of-flight channel (Fig. 2). The zero-energy scattering cross section was fixed to $\sigma_{\text{Pb}} = 11.253$ b.

Having corrected each transmission for resonance scattering, the cross sections were calculated and correct-

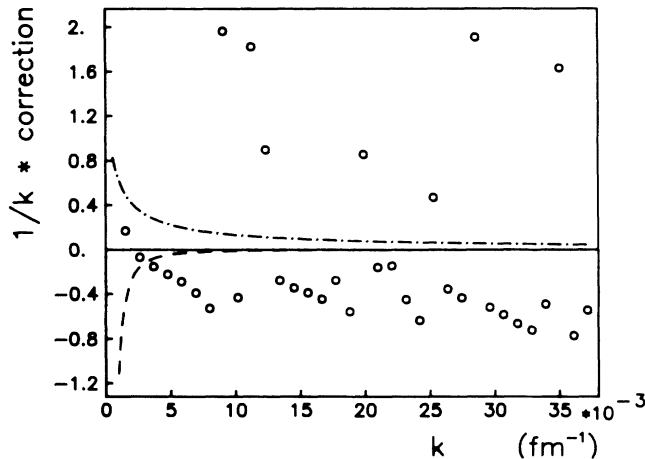


FIG. 2. Corrections to the total cross section in units of scattering cross section at $E=0$. The values are averaged and multiplied by $1/k$ to show their effect on the evaluation of the electric polarizability based on the characteristic term proportional to k in Eq. (2). The corrections due to resonance (circles), Schwinger (dashed line), and neutron-electron (dash-dotted line) scattering are shown. They can be directly compared to the data shown in Fig. 3.

ed for Schwinger and neutron-electron scattering. The evaluation of Eq. (2) for the whole set of data in the energy range from 50 eV to 20 keV (0.0015 to 0.031 fm^{-1}) yields for the shape of the total scattering cross section of lead

$$\sigma_s = 11.253(5) + 0.060(51)k - 371(27)k^2. \quad (4)$$

In the same energy range the total cross section of carbon is

$$\sigma_s = 4.7435(16) + 0.006(22)k - 82(5)k^2. \quad (5)$$

The carbon data have higher background, mainly because of the higher transmission of the time-dependent γ -ray component through the sample.

The values for the total scattering cross section of natural lead [$11.253(5)$ b] and carbon [$4.7435(16)$ b] at $k=0$ are in very good agreement with the best measured values of the total cross section if corrected for absorption, Schwinger, and neutron-electron scattering [lead¹⁰: $11.253(4)$ b and carbon¹⁷: $4.746(2)$ b]. The effective range obtained for C in Eq. (5) is in good agreement with values²² from data evaluations in a much wider energy range up to 15 MeV. That one of Pb, Eq. (4), compares favorably with values calculated for $R_0=9.73$ fm. For the carbon data the coefficient linear in k is compatible with zero. This all together provides a good test for the quality of the experiment.

From the term proportional to k in Eq. (4) the electric polarizability can be evaluated to be

$$a_n = (1.2 \pm 1.0) \times 10^{-3} \text{ fm}^3. \quad (6)$$

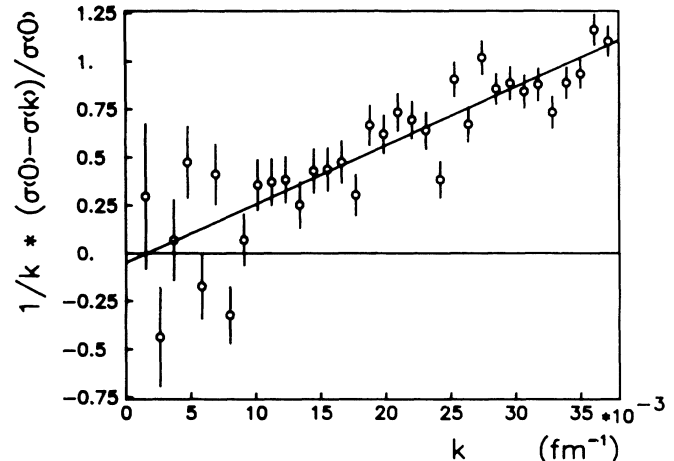


FIG. 3. Change in the corrected total scattering cross section of lead vs k as defined in Eq. (3). The slope of the straight line fitted to the experimental data results from the effective range of the nuclear potential. The electric polarizability can be obtained from the value at $k=0$.

The effect of a_n to the cross-section data can be seen in Fig. 3 in terms of Eq. (3). Systematic errors from the data reduction and resonance corrections, which were obtained with the new parameter and the appropriate negative energy levels given in Ref. 18, were estimated to be small. The errors⁷ of the neutron-electron scattering give for a_n an error well below $0.05 \times 10^{-3} \text{ fm}^3$. Even smaller are the errors by the Schwinger scattering. The quoted error in Eq. (6) is therefore mainly determined by the statistical accuracy.

Our result is in agreement with the value²³ of $a_n = (0.8 \pm 1.0) \times 10^{-4} \text{ fm}^3$ which was very recently evaluated from separate measurements of the absolute cross section of natural Pb at the distinct energies of 1.26, 5.19, 132, and 1970 eV.

In conclusion, we wish to point out that the only previous experiment²⁴ which has used the shape of total scattering cross section gave a value of $(13 \pm 8) \times 10^{-3} \text{ fm}^3$ for Bi. In the present high-precision measurement, all the relevant corrections have been determined accurately and the errors of this method were reduced drastically. For the first time the linear term in $\hbar q$ of the shape of the cross section was used explicitly and a most reliable value for a_n is obtained, which can be compared with results from various quark models.¹ In addition, if better statistics and a ^{208}Pb sample are available, the method used seems to be further capable of reducing the errors by at least a factor of 3 and thereby of setting constraints on different models. Such a new project is in progress.

We thank the Harwell nuclear physics group, Dr. M. Coates, and the HELIOS linac group for the opportunity to perform the neutron-transmission experiments. One of us (J.S.) wants to thank M. C. Moxon for numerous

discussions, his help, and for making REFIT available to us. This work was supported by the Fonds zur Förderung der Wissenschaftlichen Forschung (Projekt 5520).

¹G. Dattoli, G. Matone, and D. Prosperi, *Lett. Nuovo Cimento* **19**, 601 (1977); A. Schäfer *et al.*, *Phys. Lett.* **143B**, 323 (1984); R. Weiner and W. Weise, *Phys. Lett.* **159B**, 85 (1985).

²M. Damashek and F. J. Gilman, *Phys. Rev. D* **1**, 1319 (1970).

³J. Bernabeu and T. E. O. Ericson, *Phys. Lett.* **42**, 93 (1972).

⁴U. E. Schröder, *Acta Phys. Austriaca* **36**, 248 (1972), and *Phys. Rev. D* **12**, 896 (1975), and *Nucl. Phys.* **B166**, 103 (1980).

⁵R. M. Thaler, *Phys. Rev.* **114**, 827 (1959).

⁶G. Breit and M. L. Rustgi, *Phys. Rev.* **114**, 830 (1959).

⁷V. E. Krohn and G. R. Ringo, *Phys. Rev. D* **8**, 1305 (1973); L. Koester, W. Nistler and W. Waschkowski, *Phys. Rev. Lett.* **36**, 1021 (1976).

⁸L. Koester, *Neutron Scattering Lengths and Fundamental Neutron Interactions*, Springer Tracts in Modern Physics Vol. 80 (Springer-Verlag, Berlin, 1977).

⁹Y. A. Aleksandrov, G. S. Samosvat, Z. Sereeter, and T. G. Sor, *Pis'ma Zh. Eksp. Teor. Fiz* **4**, 196 (1966) [*JETP Lett.* **4**, 134 (1966)].

¹⁰L. Koester, W. Waschkowski, and A. Klüver, *Physica (Amsterdam)* **137B**, 282 (1986).

¹¹G. V. Anikin and I. I. Kotukhov, *Yad. Fiz.* **14**, 269 (1972) [*Sov. J. Nucl. Phys.* **14**, 152 (1972)].

¹²J. Schmiedmayer, Ph.D thesis, Technical University Vien-

na, 1987 (unpublished); J. Schmiedmayer *et al.*, to be published.

¹³V. F. Sears, *Phys. Rep.* **141**, 281-317 (1986).

¹⁴J. H. Hubbel *et al.*, *J. Phys. Chem. Ref. Data* **4**, 471 (1975).

¹⁵H. Leeb, G. Eder, and H. Rauch, *J. Phys. (Paris), Colloq.* **45**, C3-47 (1984).

¹⁶J. Schmiedmayer, M. Pernicka, and M. C. Moxon, to be published.

¹⁷*Neutron Cross Sections Part A: Z=10*, edited by S. F. Mughabghab, M. Divadeenam, and N. E. Holden (Academic, New York, 1983), Vol. 1; *Neutron Cross Sections, Part B: Z=61-100*, edited by S. F. Mughabghab (Academic, New York, 1985), Vol. 1.

¹⁸M. J. Martin, *Nucl. Data Sheets* **47**, 797 (1986).

¹⁹J. Schmiedmayer, to be published.

²⁰M. C. Moxon, REFIT program description, unpublished. In REFIT the Doppler-broadened neutron-nucleus cross section is calculated with a multi-level *R*-matrix formalism. The calculated transmission is convoluted with the time-of-flight resolution function as obtained from the initial pulse shape, target pulse decay, moderation time jitter, geometry effects, and detector time resolution. A minimizing routine is used to determine the best fit to the experimental data by variation of selected parameters.

²¹H. Schumacher *et al.*, *Phys. Status Solidi* **20**, 109 (1973).

²²H. T. Heaton *et al.*, *Nucl. Sci. Eng.* **56**, 27 (1975); J. C. Lachkar, in *Symposium on Neutron Standards and Applications*, edited by C. D. Bowman, A. D. Carlson, H. O. Liskien, and L. Stewart, National Bureau of Standards Special Publication No. 439 (U.S. GPO, Washington, DC, 1977), p. 93.

²³L. Koester, W. Waschkowsky, and J. Meier, *Z. Phys. A* **329**, 229 (1988).

²⁴Y. A. Aleksandrov, *Yad. Fiz.* **38**, 1100 (1983) [*Sov. J. Nucl. Phys.* **38**, 660 (1983)].